Research Article | Vol. 25, No. 14 | 10 Jul 2017 | OPTICS EXPRESS 16017
Optics EXPRESS

Performance of adaptive DD-OFDM multicore fiber links and its relation with intercore crosstalk

TIAGO M. F. ALVES,[1,*] RUBEN S. LUÍS,[2] BENJAMIN J. PUTTNAM,[2] ADOLFO V. T. CARTAXO,[1,3] YOSHINARI AWAJI,[2] AND NAOYA WADA[2]

[1]*Instituto de Telecomunicações, 1049-001 Lisbon, Portugal*
[2]*Photonic Network System Laboratory, National Institute of Information and Communication Technology, Tokyo 184-8759, Japan*
[3]*ISCTE - Instituto Universitário de Lisboa, 1649-026 Lisbon, Portugal*
[*]*tiago.alves@lx.it.pt*

Abstract: Adaptive direct-detection (DD) orthogonal frequency-division multiplexing (OFDM) is proposed to guarantee signal quality over time in weakly-coupled homogenous multicore fiber (MCFs) links impaired by stochastic intercore crosstalk (ICXT). For the first time, the received electrical power of the ICXT and the performance of the adaptive DD-OFDM MCF link are experimentally monitored quasi-simultaneously over a 210 hour period. Experimental results show that the time evolution of the error vector magnitude due to the ICXT can be suitably estimated from the normalized power of the detected crosstalk. The detected crosstalk results from the beating between the carrier in the test core and ICXT originating from the carrier and modulated signal from interfering core. The results show that the operation of DD-OFDM systems employing fixed modulation can be severely impaired by the presence of ICXT that may unpredictable vary in both power and frequency. The system may suffer from deleterious impact of moderate ICXT levels over a time duration of several hours or from peak ICXT levels occurring over a number of minutes. Such power fluctuations can lead to large variations in bit error ratio (BER) for static modulation schemes. Here, we show that BER fluctuations may be minimized by the use of adaptive modulation techniques and that in particular, the adaptive OFDM is a viable solution to guarantee link quality in MCF-based systems. An experimental model of an adaptive DD-OFDM MCF link shows an average throughput of 12 Gb/s that represents a reduction of only 9% compared to the maximum throughput measured without ICXT and an improvement of 23% relative to throughput obtained with static modulation.

OCIS codes: (060.2330) Fiber optics communications; (060.0060) Fiber optics and optical communications.

References and links

1. T. Morioka, "New generation optical infrastructure technologies: "EXAT Initiative" towards 2020 and beyond," in *OptoElectronics and Communications Conference*, Technical Digest Series (CD) (2009), paper FT4.
2. D. Richardson, J. Fini, and L. Nelson, "Space-division multiplexing in optical fibres," Nat. Photon. **7**, 354–362 (2013).
3. B. J. Puttnam, R. S. Luís, W. Klaus, J. Sakaguchi, J. Mendinueta, Y. Awaji, N. Wada, Y. Tamura, T. Hayashi, M. Hirano, and J. Marciante, "2.15 Pb/s transmission using a 22 core homogeneous single-mode multi-core fiber and wideband optical comb," *European Conference on Optical Communications*, Technical Digest Series (CD) (2015), paper PDP.3.1.
4. T. Kobayashi, H. Takara, A. Sano, T. Mizuno, H. Kawakami, Y. Miyamoto, K. Hiraga, Y. Abe, H. Ono, M. Wada, Y. Sasaki, I. Ishida, K. Takenaga, S. Matsuo, K. Saitoh, M. Yamada, H. Masuda, and T. Morioka, "2×344 Tb/s propagation-direction interleaved transmission over 1500-km MCF enhanced by multicarrier full electric-field digital back-propagation," *European Conference on Optical Communications*, Technical Digest Series (CD) (2013), paper PD3.E.4.
5. B. J. Puttnam, R. S. Luís, T. Eriksson, W. Klaus, J. Mendinueta, Y. Awaji, and N. Wada, "Impact of intercore crosstalk on the transmission distance of QAM formats in multicore fibers," Photon. J. **8**(2), 0601109 (2016).
6. T. Eriksson, B. J. Puttnam, R. S. Luís, M. Karlsson, P. Andrekson, Y. Awaji, and N. Wada, "Experimental investigation of crosstalk penalties in multicore fiber transmission systems," Photon. J. **7**(1), 7200507 (2015).

#291846 https://doi.org/10.1364/OE.25.016017
Journal © 2017 Received 30 Mar 2017; revised 26 May 2017; accepted 29 May 2017; published 28 Jun 2017

Optics EXPRESS

7. T. Hayashi, T. Taru, O. Shimakawa, T. Sasaki, and E. Sasaoka, "Design and fabrication of ultra-low crosstalk and low-loss multi-core fiber," Opt. Express **19**(17), 16576–16592 (2011).
8. A. Cartaxo and T. Alves, "Discrete changes model of inter-core crosstalk of real homogeneous multi-core fibers," J. Lightwave Technol. **35**(12), 2398–2408 (2017).
9. R. S. Luís, B. J. Puttnam, A. Cartaxo, W. Klaus, J. Mendinueta, Y. Awaji, N. Wada, T. Nakanishi, T. Hayashi, and T. Sasaki, "Time and modulation frequency dependence of crosstalk in homogeneous multi-core fibers," J. Lightwave Technol. **34**(2), 441–447 (2016).
10. T. Alves and A. Cartaxo, "Theoretical modelling of random time nature of inter-core crosstalk in multicore fibers," *IEEE Photonics Conference*, Technical Digest Series (CD) (2016), paper WB2.4.
11. J. Pedro, R. S. Luís, B. J. Puttnam, Y. Awaji, N. Wada, and A. Cartaxo, "Experimental assessment of the time-varying impact of multi-core fiber crosstalk on a SSB-OFDM signal," in *Photonics in Switching*, Technical Digest Series (CD) (2015), 166–168.
12. J. He, B. Li, L. Deng, M. Tang, L. Gan, S. Fu, P. Shum, and D. Liu, "Experimental investigation of inter-core crosstalk of MIMO-OFDM/OQAM radio over multicore fiber system," Opt. Express **24**(12), 13418–13428 (2016).
13. J. Sakaguchi, B. J. Puttnam, W. Klaus, Y. Awaji, N. Wada, A. Kanno, T. Kawanishi, K. Imamura, H. Inaba, K. Mukasa, R. Sugizaki, T. Kobayashi, and M. Watanabe, "305 Tb/s space division multiplexed transmission using homogeneous 19-core fiber," J. Lightwave Technol. **31**(4), 554–562 (2013).
14. G. Rademacher, B. J. Puttnam, R. Luís, Y. Awaji, and N. Wada, "Time-dependent crosstalk from multiple cores in a homogeneous multi-core fiber," in Optical Fiber Communication Conference, OSA Technical Digest (Optical Society of America, 2017), paper Th1H.3.

1. Introduction

Space-division multiplexing systems based on multicore fibers (MCFs) show a high potential to overcome the expected capacity crunch in optical fiber networks [1,2]. MCF-based transmission records with a capacity per fiber of 2.15 Pb/s [3] or a capacity-distance product of 1.032 Eb/s·km [4] have been demonstrated. These proof-of-concept experiments were demonstrated under low-intercore crosstalk (ICXT) levels. However, moderate or high ICXT levels may have an increasingly detrimental impact on the transmission distance and performance achieved by MCF-based systems [5, 6].

Over the last years, simple theoretical models to estimate the ICXT variation along the longitudinal direction of weakly-coupled MCFs were proposed [7,8]. The performance of MCF-based systems may be also significantly affected by the dynamic behavior of the ICXT [5]. Weak mode coupling in real single-mode homogeneous MCFs leads to accumulation of ICXT that may induce time and frequency dependent performance degradation [9, 10]. In [9], theoretical expressions of the mean and variance of the crosstalk transfer function (XTTF) amplitude were derived, and spectrograms of the XTTF amplitude and the time evolution of the short-term average crosstalk (STAXT) were experimentally measured. Variations of the STAXT along time of 10 dB and XTTF amplitude fluctuations along time and frequency exceeding 15 dB were observed in experimental measurements taken over a 10 hour period [9]. The impact of these STAXT and XTTF variations on a system performance was first addressed in [11]. There, the performance of an MCF-based direct-detection (DD) orthogonal frequency division multiplexing (OFDM) system employing fixed modulation was monitored over 36 hours. Recently, the impact of the ICXT on the performance of a multiple input-multiple output OFDM radio over 7-core MCF system employing 16 quadrature amplitude modulation (QAM) was also investigated [12]. Remarkable performance penalties induced by the ICXT were experimentally shown in [11, 12]. The works reported in [11, 12] have confirmed that MCF systems impaired by moderate to strong ICXT can have substantial performance variation, following the stochastic behavior of ICXT. For fixed modulation schemes, this may result in critical outage probabilities that may discourage the deployment of MCF systems, as suggested by [9, 11]. In contrast, adaptive modulation formats have the potential to reduce the impact of the ICXT on the MCF system performance and improve the achievable throughput. Adaptive systems may exploit the random time nature of the ICXT to adjust and optimize the system throughput along time while ensuring operation with acceptable outage probabilities due to

Optics EXPRESS

ICXT.

In this work, an adaptive DD-OFDM-based weakly-coupled homogeneous MCF link impaired by moderate stochastic ICXT is experimentally demonstrated. The ICXT and performance of the MCF link are monitored quasi simultaneously over a 210 hour period. It is shown that the time varying error vector magnitude (EVM) of the DD-OFDM system, limited by the ICXT, may be suitably estimated by the time evolution of the beating between the optical carrier and the ICXT originating from the carrier and OFDM signal launched into neighboring cores. A tolerance to large ICXT fluctuations in such an adaptive DD-OFDM system is shown. An average throughput of 12 Gb/s, that represents a reduction of only 9% relative to the throughput achieved without ICXT and an improvement of 23% relative to throughput obtained with static modulation, is measured.

2. Detected ICXT in DD-OFDM systems

In this section, the detected ICXT in MCF systems employing DD-OFDM is derived and discussed. Two cores are considered in the analysis: (i) the interfering core is used to generate the crosstalk signal, and (ii) the test core is used to evaluate the ICXT and its impact on the OFDM signal performance. It is assumed that the signals transmitted in the two cores have similar spectral occupancy.

In the case of a DD-OFDM system, the core coupling creates a ICXT signal in the test core with the spectral content located mainly in two regions: (i) a low-frequency region, whose spectral content is due to the ICXT induced by the optical carrier (OC) of the interfering core, and (ii) a bandpass frequency region, whose spectral content is due to the ICXT induced by the data signal transmitted in the interfering core. Considering that the signal of the test core is polarized in the $\mathbf{u_x}$ direction and the ICXT signal is unpolarized, and taking the polarization of the signal of the test core as a reference, the Jones vector of the optical signal at the output of the test core, $\mathbf{e_o}(t)$, can be expressed as:

$$\mathbf{e_o}(t) = [A_{t,x} + s_{t,x}(t) + A_{XT,x}(t) + s_{XT,x}(t)]\mathbf{u_x} + [A_{XT,y}(t) + s_{XT,y}(t)]\mathbf{u_y} \quad (1)$$

where $A_{t,x}$ and $s_{t,x}(t)$ are the OC and data signal of test core, respectively. $A_{XT,a}(t)$ and $s_{XT,a}(t)$ are the ICXT components originating from the OC and data signal of interfering core, respectively, in polarization direction $\mathbf{u_a}$ (with $a = x$ or $a = y$). A scheme illustrating the spectral content of the different terms of Eq. (1) is shown in Fig. 1. The electrical current

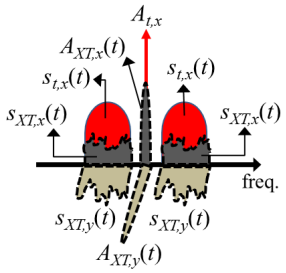

Fig. 1. Illustration of the spectral content of the signal and ICXT terms at the output of the test core.

Optics EXPRESS

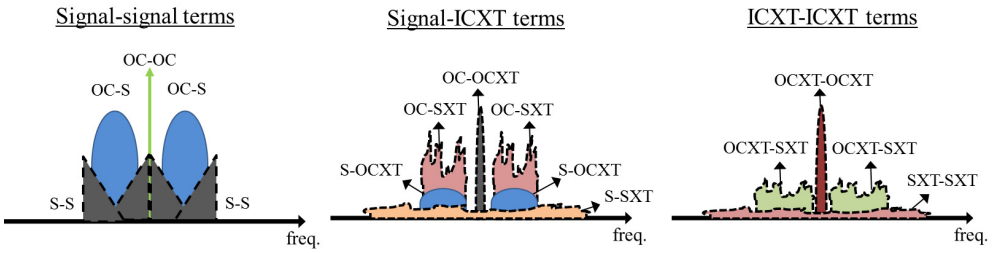

Term	Description	Term	Description
OC-OC	Out-of-band	S-OCXT	Distorted replica of data signal (equalized in OFDM receiver)
OC-S	Data signal	OCXT-OCXT	Out-of-band ICXT
S-S	Signal-signal beat interference	OCXT-SXT	Negligible ICXT
OC-OCXT	Out-of-band	SXT-SXT	Negligible ICXT
OC-SXT	In-band ICXT		

Fig. 2. Illustration of the spectral content of the terms of Eq. 2 and description of their impact on the received data signal.

resulting from square law detection of the signal in the test core is given by:

$$\begin{aligned}\frac{i(t)}{R_\lambda} = &\underbrace{|A_{t,x}|^2}_{\text{OC-OC}} + \underbrace{2\Re\{A_{t,x}s^*_{t,x}(t)\}}_{\text{OC-S}} + \underbrace{|s_{t,x}(t)|^2}_{\text{S-S}} + \\ &+ 2\Re\{\underbrace{A_{t,x}A^*_{XT,x}(t)}_{\text{OC-OCXT}} + \underbrace{A_{t,x}s^*_{XT,x}(t)}_{\text{OC-SXT}} + \underbrace{s_{t,x}(t)\,A^*_{XT,x}(t)}_{\text{S-OCXT}} + \underbrace{s_{t,x}(t)\,s^*_{XT,x}(t)}_{\text{S-SXT}}\} + \\ &+ \underbrace{|A_{XT,x}(t)|^2}_{\text{OCXT-OCXT}} + \underbrace{2\Re\{A_{XT,x}(t)\,s^*_{XT,x}(t)\}}_{\text{OCXT-SXT}} + \underbrace{|s_{XT,x}(t)|^2}_{\text{SXT-SXT}} + \\ &+ \underbrace{|A_{XT,y}(t)|^2}_{\text{OCXT-OCXT}} + \underbrace{2\Re\{A_{XT,y}(t)\,s^*_{XT,y}(t)\}}_{\text{OCXT-SXT}} + \underbrace{|s_{XT,y}(t)|^2}_{\text{SXT-SXT}}\end{aligned} \quad (2)$$

where z^* stands for the conjugate of z, R_λ is the PIN responsivity and $\Re\{x\}$ is the real part of x. Equation (2) allows grouping of the detected ICXT in two main sets of terms: (i) the beating between the signal (OC and data signal) transmitted in the test core and the ICXT (terms in the second line of Eq. (2)), and (ii) the beating between the ICXT components originating from the OC and data signal of x and y polarizations (terms in the third and fourth lines of Eq. (2)). The terms of the first line of Eq. (2) are due to the beating between the OC and data signal of the test core, and comprise the OC beating (OC-OC), the desired signal that results from the beating between the OC and the data signal (OC-S), and the signal-signal beat interference (S-S).

Figure 2 illustrates the spectral content of the different terms of Eq. (2). The description of the impact of each term on the received data signal is also presented. Figure 2 shows that, after photodetection, the data signal is impaired mainly by two in-band ICXT terms. (i) The term that results from the beating between the ICXT originating from the data signal of the interfering core and the OC transmitted in the test core (OC-SXT beating). (ii) A term originated from the signal modulation in the interfering core and that results from the beating between the ICXT originating from the OC with the ICXT originating from the data signal (OCXT-SXT beating).

Optics EXPRESS

The XTTF defined in [9] can be obtained from this OCXT-SXT term if a sinusoidal signal is considered at the input of the interfering core. In systems with similar optical power levels launched into each core, A_t is much higher than $A_{XT}(t)$ and the OC-SXT term is expected to dominate over the OCXT-SXT term. However, further analysis concerning the impact of the polarization effect on the beating between the signals of each term is still required and left for a future work.

The beating between the ICXT originating from the OC of the interfering core and the data signal transmitted in the test core (S-OCXT beating), the beating between the data signal of the test core and the ICXT originating from the data signal transmitted in the interfering core (S-SXT beating), and the beating of the ICXT originating from the data signal with itself (SXT-SXT beating) also present some in-band spectral content. As the time variation of the ICXT originating from the OC is usually much slower than the time variation of the data signal, the S-OCXT term is proportional to the data signal with the proportionality constant having a random amplitude and phase induced by the ICXT originating from the OC that changes much more slowly in time than the symbol duration of the data signal and therefore can be easily removed by the OFDM equalizer. In the case of the S-SXT term, as the power of the OC dominates over the power of the data signal in the test core (as it is the case of most DD-OFDM systems), the power of this term is usually much lower than the power of the OC-SXT beating. The power of the SXT-SXT term is also negligible because the power of the OC is usually much higher than the data signal power. The power of the ICXT originating from the OC created in the test core in the absence of electrical signal modulation and without launching a signal into the test core (OCXT-OCXT beating) and the beating between the OC transmitted in the test core and the ICXT originating from the OC (OC-OCXT) are located at very low-frequency and are out-of-band of the OFDM signal. We stress that the OCXT-OCXT beating term corresponds to the STAXT measured experimentally in [9].

In summary and assuming that the spectrum location of the OFDM data signal is slightly away from DC, we conclude that the detected ICXT can be approximated by:

$$\frac{i_{XT}(t)}{R_\lambda} \approx 2\Re\{A_{t,x}s^*_{XT,x}(t) + A_{XT,x}(t)\,s^*_{XT,x}(t) + A_{XT,y}(t)\,s^*_{XT,y}(t)\} \tag{3}$$

Equation (3) shows that the detected ICXT in DD-OFDM systems can be estimated by launching the signal into the interfering core and the OC in the test core to assist the ICXT detection.

The analysis of this section assumed that the signals transmitted in the two cores have similar spectral occupancy. If the DD-MCF-based system is designed to have the signals launched into the interfering cores with a spectral occupancy different from that of the signal launched into the test core, then it is expected that the impact of the ICXT on the performance of the signal launched into the test core is significantly decreased.

3. Experimental setup

Figure 3 shows the setup used to measure the ICXT and the performance of the adaptive DD-OFDM MCF system. The MCF is a 10.1 km-long homogeneous trench-assisted 19-core fiber with the profile shown in the inset (i), cladding diameter of 200 μm, core pitch of 35 μm, coating diameter of 345 μm, average loss of 0.23 dB/km and mean ICXT of -32 dB [13]. Depending on the type of measurements, the following three setup configurations are used along this work.

3.1. Configuration 1: STAXT

This configuration is used to take experimental measurements of the STAXT introduced in section 2. This is accomplished by switching off the frequency synthesizer and the arbitrary waveform generator (AWG) shown in Fig. 3, and by launching only the OC in the interfering

Optics EXPRESS

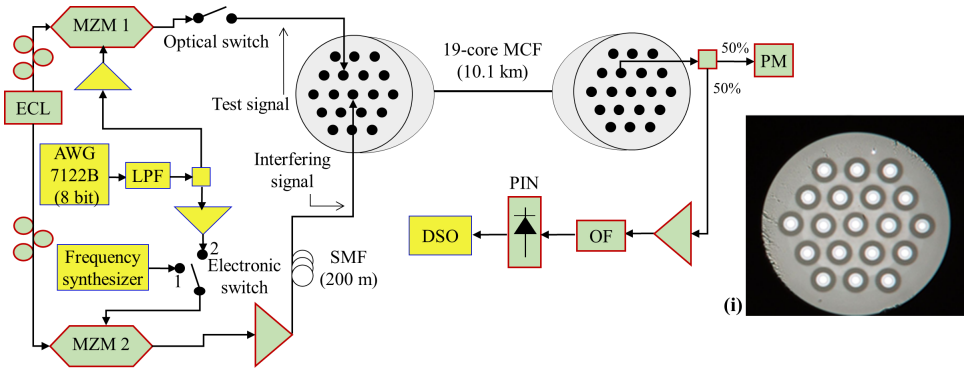

Fig. 3. Experimental setup used to measure the ICXT and the performance of adaptive DD-OFDM-based MCF systems. (i) 19-core MCF profile. AWG: arbitrary waveform generator; DSO: digital storage oscilloscope; ECL: external cavity laser; LPF: low-pass filter; MZM: Mach-Zehnder modulator; OF: optical filter; PIN: positive-intrinsic-negative; PM: power meter; SMF: single-mode fiber.

core. The OC is generated from an external cavity laser (ECL) operating at 1552.52 nm and a single-arm Mach-Zehnder modulator (MZM) biased 6 dB below the maximum power of their input-output characteristic, and the power at the interfering core input is 10 dBm. The STAXT is then measured by using a power meter at the output of the test core.

3.2. Configuration 2: detected ICXT

The main target of this configuration is to realize experimental measurements of the detected ICXT expressed by Eq. (3). As the terms of the detected ICXT arising from the data signal, $s_i(t)$, are negligible, only the OC is launched into the test core. To obtain the frequency dependence of the detected ICXT, we use a frequency synthesizer (electronic switch in position 1) to transmit a sinusoidal signal, the frequency of which is swept along the bandwidth of the OFDM signal (between 200 MHz and 2.7 GHz). Power loading is employed in the generator to remove the limited frequency response of the electrical circuitry. The interfering optical signal is generated using the ECL and a single-arm MZM. This modulator (MZM 2 in Fig. 3) as well as MZM 1 are biased 6 dB below the maximum power of their input-output characteristic to avoid significant signal-signal beat interference. The power of the OC at the interfering core input is 10 dBm. The power of the OC injected in the test core is -3.5 dBm. The higher power of the interfering core is required to obtain measurable detected ICXT power levels. In the optical receiver, optical pre-amplification is used to increase the signal power at the PIN input. An optical filter with a bandwidth of 0.15 nm to reduce noise power and a 16 GHz PIN photodetector are used. The sinusoidal signal is captured by a 12 GHz oscilloscope.

3.3. Configuration 3: OFDM performance

This configuration enables evaluating the impact of the time-varying ICXT on the performance of the adaptive DD-OFDM system. An AWG operating at 20 Gsamples/s generates an OFDM signal with a bandwidth of 2.5 GHz and centered at 1.45 GHz. The OFDM signal consists of 1000 data symbols and 100 training symbols. Each OFDM symbol consists of 128 subcarriers and different symbols are used in each of several separate measurements. The OFDM signal from the AWG is split in two to create the test and interfering signals, amplified and applied to MZM 1 and MZM 2 (electronic switch in position 2). A single-mode fiber with 200 m (corresponding to a time lag of 20 OFDM symbols) is used at the interfering core input to decorrelate the two signals. The power launched into the test core is -3.5 dBm with 10 dBm

Optics EXPRESS

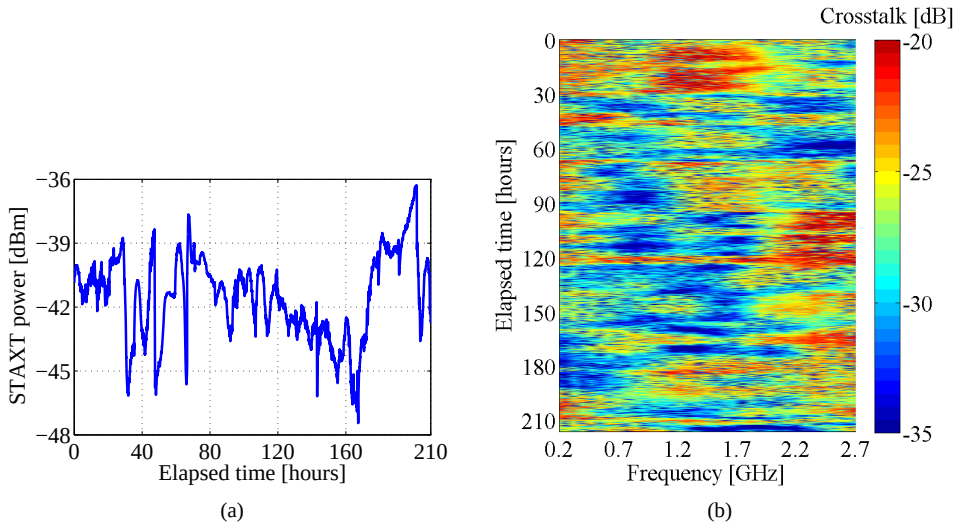

Fig. 4. (a) STAXT power at the 19-core MCF output measured continuously over a 210 hour period. (b) Spectrogram of the normalized power of the detected ICXT measured along the 210 hour in the bandwidth of the OFDM signal.

launched into the interfering core to emulate a link affected by moderate ICXT. After the optical receiver, the OFDM signal is captured by a 12 GHz oscilloscope and digitized at 20 Gsamples/s. Offline processing is used for OFDM frame synchronization, cyclic prefix extraction, fast Fourier transform, one-tap frequency domain equalization and performance assessment.

As this work is a first proof-of-concept of the tolerance of adaptive OFDM to the ICXT generated in MCF links, only a simple bit loading scheme is employed: (i) the EVM per subcarrier is evaluated from the training symbols with 16-QAM mapping and (ii) modulation formats (4, 16, 32 or 64-QAM) for every subcarrier are evaluated targeting a bit error ratio (BER) of $10^{-2.4}$ corresponding to the two interleaved extended BCH(1020,988) 7% forward error correction (FEC) codes threshold (ITU-T G.975.1 rec.). Potential performance improvements achieved with other more complex adaptive schemes are left for future studies.

4. Results

The STAXT, detected ICXT and performance of the OFDM signal were measured quasi simultaneously. Each set of measurements (STAXT, detected ICXT and performance) were taken at 2.1 minute intervals over a 210 hour period (more than 8 days). To the best of our knowledge, this is the longest reported time period over which an ICXT-impaired direct-detection MCF link has been continuously monitored. Successive measurements taken at 2.1 minutes were deemed sufficient to capture small fluctuations of ICXT power and performance between consecutive measurements due to the large ICXT decorrelation time of the cores under analysis (more than 2 hours).

4.1. STAXT and detected ICXT

Figure 4(a) depicts the STAXT power measured over the 210 hour period. Figure 4(a) shows STAXT power fluctuations over time that exceed 10 dB. These fluctuations are characterized by unexpected behaviors that include a STAXT power variation only of around 2 dB in the first 20 hours of measurements and variations that may exceed 7 dB in a time interval with duration as low as 20 minutes as observed close to hours 30, 47, 66 or 202. In MCF-based systems with

Optics EXPRESS

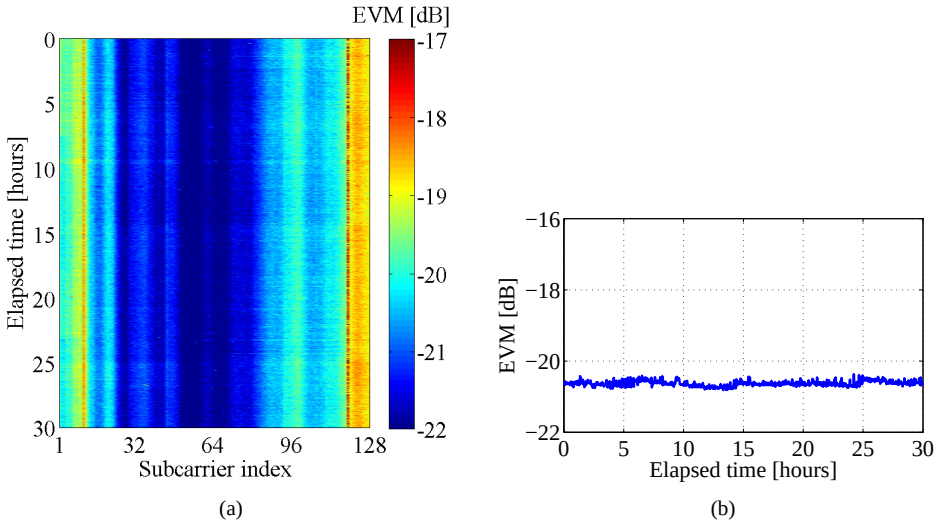

Fig. 5. (a) Spectrogram of the EVM of the adaptive OFDM signal transmitted in the test core without ICXT. (b) Average EVM of the adaptive OFDM signal transmitted in the test core without ICXT.

more cores being excited, an increase of the STAXT power and of the speed of the STAXT fluctuations is expected [14].

Figure 4(b) depicts the spectrogram of the normalized power of the detected ICXT when a sinusoidal signal is injected in the interfering core. The normalization factor is the power of the detected signal when no signal is launched into the interfering core and a low-frequency sinusoidal signal is injected in the test core. Similar spectrograms of the ICXT were reported also in [9]. However, the analysis of that work was focused on the XTTF which is obtained only from the ICXT components. Figure 4(b) suggests that OFDM subcarriers may be affected by the random detected ICXT fluctuations that occur over a 15 dB range. These fluctuations may lead to unacceptable outage probabilities in a significant part of the OFDM subcarriers when fixed modulation is used.

4.2. OFDM performance

We started the analysis of the MCF-based OFDM system by measuring the performance of the adaptive OFDM signal transmitted in the test core without launching signal into the interfering core, i. e., in the absence of ICXT. Figure 5(a) shows the spectrogram of the EVM of the OFDM signal of test core in the absence of ICXT. An EVM degradation, relative to the center subcarriers, that achieves 3 dB and 4 dB for the subcarriers with the lower and higher indexes, respectively, is shown. The worst EVM is observed in the subcarriers with lower indexes (located at lower frequencies) which results from the power of the signal-signal beat interference. For the subcarriers with higher indexes, the EVM degradation occurs mainly due to the limited bandwidth of the electronics used in the setup. Figure 5(b) depicts the temporal evolution of the average EVM of the adaptive OFDM signal of the test core calculated over all the subcarriers without ICXT. These measurements show a stable average EVM close to -20.5 dB along the 30 hour period in the absence of ICXT.

Figure 6(a) shows the measured spectrogram of the EVM of the adaptive OFDM signal in the test core when an OFDM signal is also launched into the interfering core. A qualitative comparison between the EVM shown in Fig. 6(a) and the detected ICXT spectrogram of Fig. 4(b) reveals that the performance degradation of the DD-OFDM system occurs in time

Optics EXPRESS

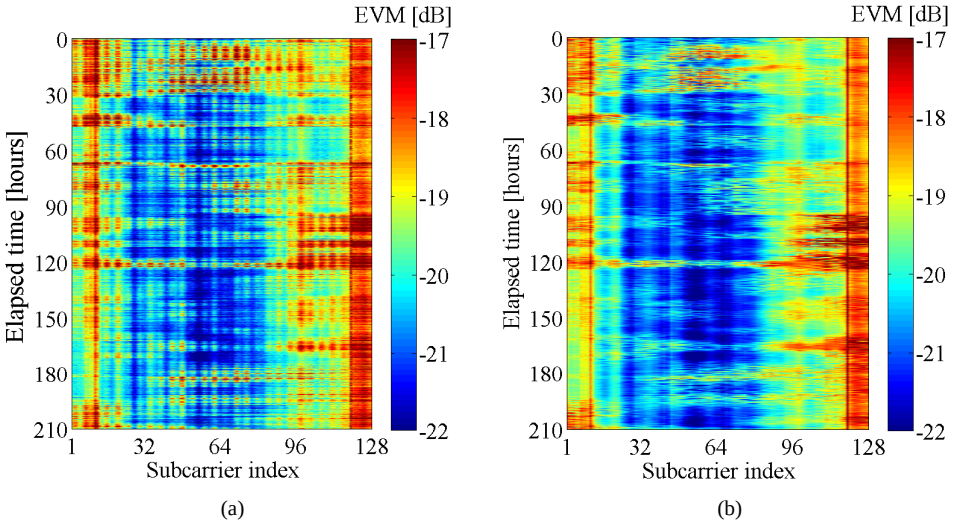

Fig. 6. (a) Measured spectrogram of the EVM of the adaptive OFDM signal transmitted in the test core. (b) Spectrogram of the EVM of the adaptive OFDM signal transmitted in the test core estimated from the measured detected ICXT and measured EVM in the absence of ICXT.

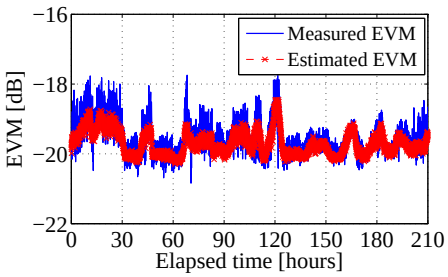

Fig. 7. Measured and estimated average EVM of the adaptive OFDM signal transmitted in the test core.

intervals where OFDM subcarriers are affected by higher levels of detected ICXT. To confirm if this similar qualitative behavior also translates into a quantitative relation, the EVM estimated from adding the measured normalized power of the detected ICXT and the measured EVM in the absence of ICXT was obtained. Figure 6(b) shows the result of this EVM obtained by adding the EVM in the absence of ICXT shown in Fig. 5(a) and the measurements of the normalized power of the detected ICXT depicted in Fig. 4(b). The comparison between Fig. 6(a) and Fig. 6(b) shows very good agreement between the measured EVM and the EVM estimated from the normalized power of the detected ICXT and confirms that the performance of DD-OFDM MCF links dominantly impaired by the ICXT is closely related to the detected ICXT defined by Eq. (3).

Although these results have been obtained with only one interfering core, we expect that the EVM can be also adequately characterized from the normalized power of the detected ICXT when MCFs with multiple excited cores are considered as the detected ICXT includes all the ICXT contributions of the different excited cores.

Figure 7 depicts the measured EVM and the EVM estimated from the normalized power

of the detected ICXT over the 210 hour period. The measured EVM results are obtained by calculating the average of the EVM over all the subcarriers of the OFDM signal transmitted in the test core. Figure 7 shows temporal fluctuations of the average EVM exceeding 2 dB due to the time-varying ICXT. It shows that the time evolution of the measured EVM is quite well estimated by the EVM obtained from the temporal evolution of the normalized power of the detected ICXT. In contrast, analysis of Fig. 7 and Fig. 4(a) suggests that the performance of the DD-OFDM system is not completely characterized by the STAXT. For example, Fig. 4(a) shows that the highest peak of the STAXT power occurs close to the end of the measurement period. However, this STAXT peak does not correspond to the worst performance of the OFDM signal measured along the 210-hour period. Figure 7 shows that the worst EVM level was measured after 120 hours of measurements. At that time, the measured STAXT power is far from the peak STAXT, as shown by Fig. 4(a).

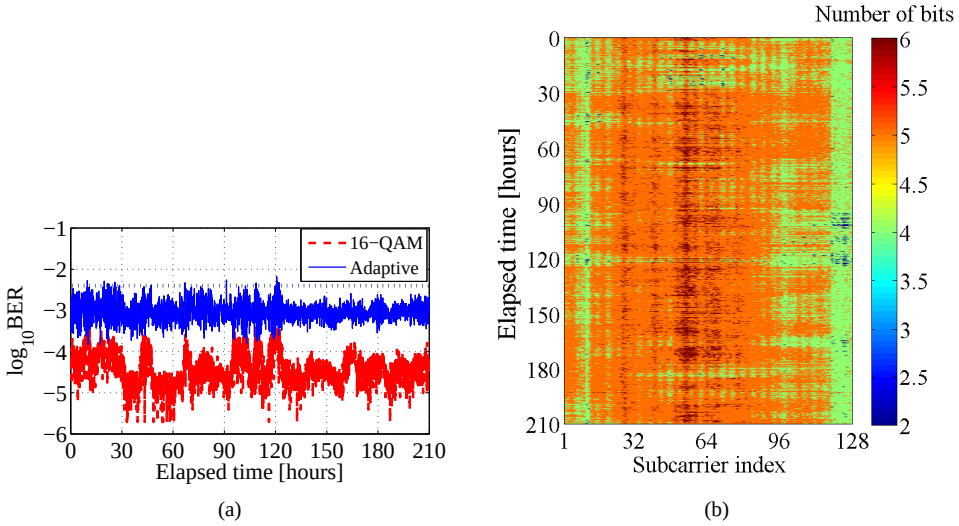

Fig. 8. (a) Time evolution of the average BER of the OFDM signal transmitted in the test core in the presence of ICXT using fixed and adaptive QAM modulations. (b) Spectrogram of the number of bits in each subcarrier of the adaptive OFDM signal. In (a), the dotted line represents the BER threshold corresponding to 7% FEC.

Figure 8(a) presents the time evolution of the average BER of the OFDM signal using fixed and adaptive QAM modulations. When all OFDM subcarriers are modulated with 16-QAM signals, large BER fluctuations are clearly observed in time instants where the detected ICXT is high. As these fluctuations induced by the ICXT are random and unpredictable, network providers cannot assure the signal quality, and the deployment of MCF links with fixed modulation is severely compromised. In contrast, the adaptive OFDM solution reveals improved tolerance to the distortion caused by the ICXT and enables to obtain a BER that rarely exceeds the $10^{-2.4}$ threshold over the 210 hour period, as initially targeted. In the case of the pair of cores under analysis, this is achieved by using the number of bits in each subcarrier with the time evolution shown in Fig. 8(b). It is clear that the subcarriers less affected by the detected ICXT are able to support QAM orders with higher spectral efficiency. These results were obtained considering only one interfering core. In the case of MCF-based systems with more interfering cores, the speed of the ICXT fluctuations increases [14] and the use of adaptive modulation to improve the tolerance of the system performance to the ICXT is still more critical.

Figure 9 shows the time variation of the throughput of the adaptive OFDM signal impaired

Optics EXPRESS

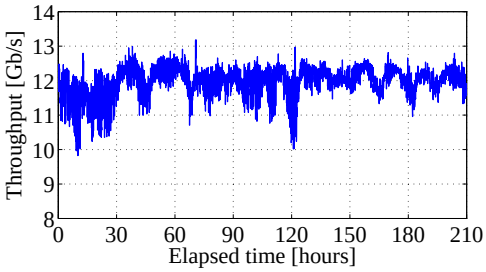

Fig. 9. Time evolution of the throughput of the adaptive OFDM signal in the presence of ICXT.

by the ICXT. Figure 9 shows a minimum throughput of 9.8 Gb/s and a peak of 13.2 Gb/s. The EVM of the OFDM signal corresponding to the peak throughput situation is -20.4 dB, i. e., this throughput is achieved in a situation where the impact of the ICXT on the performance is negligible. Without adaptive modulation, the lowest throughput achieved in the 210 hour period would be the required throughput a static modulation scheme would need to be dimensioned for in order to operate without impairment in the measured time period. As the average throughput of the adaptive OFDM system along the 210 hour period is 12 Gb/s, a throughput improvement relative to the static modulation system of 23% is achieved. It can be also concluded from this average throughput that the adaptive DD-OFDM MCF-based link can be deployed with high tolerance to random ICXT with a throughput reduction of only 9% relative to the throughput achieved by a similar system in the absence of ICXT.

5. Conclusion

A DD-OFDM system employing adaptive modulation to enable the implementation of weakly-coupled homogeneous MCF links impaired by stochastic intercore crosstalk has been experimentally demonstrated and monitored quasi-simultaneously over 210 hours for the first time. The average throughput of the adaptive OFDM system has been evaluated and compared with the throughput achieved by a similar system in the absence of ICXT and by a static modulation system.

Experimental measurements have shown that the time evolution of the EVM of the OFDM signal can be suitably estimated from the normalized power of the detected ICXT that results from the beating between the ICXT components originating from the OC and the OFDM signal launched into the interfering core and the optical carrier of the test core. Remarkably different ICXT behaviors along the measurement period have been observed with moderate ICXT levels occurring in a time duration of several hours or high peak ICXT levels occurring over a number of minutes. These variations are unpredictable due to the random time nature of ICXT and potentially can severely compromise the operation of ICXT-impaired DD-OFDM systems employing fixed modulation. In contrast, the adaptive OFDM solution has shown improved tolerance to the interference caused by the ICXT over the 210 hour period. The adaptive DD-OFDM MCF link has shown an average throughput of 12 Gb/s which represents a reduction of only 9% relative to the throughput achieved without ICXT and an improvement of 23% relative to the throughput achieved by a static modulation system.

Funding

Fundação para a Ciência e a Tecnologia (FCT) (AMEN-UID/EEA/50008/2013, IF/01225/2015/CP1310/CT0001); Instituto de Telecomunicações (AMEN-UID/EEA/50008/2013).